Rearrangement of the Aggregation of the Gelator during Sol−Gel Transcription of a Dimeric Cholesterol-Based Viologen Derivative into Fibrous Silica

Pengchong Xue, Ran Lu,* Dongmei Li,† Ming Jin, Chunyan Bao, Yingying Zhao, and Zongmu Wang‡

College of Chemistry, Jinlin University, Changchun 130023, People's Republic of China

Received September 16, 2003. Revised Manuscript Received February 17, 2004

New dimeric cholesterol-based viologen derivative **1** has been prepared and can form a very stable supergel in 1-butanol. To characterize the aggregation mode of **1** in the organogel phase, transmission electron microscopy (TEM) images, small-angle X-ray diffraction (SAXRD) patterns, and circular dichroism (CD) spectra were obtained. The TEM images show that **1** assembles into a fibrous structure composed of thin fibers with 10 nm diameters, which are derived from two twist unimolecular stacking fibers, and the dipole moments tend to orient in a clockwise direction as shown in the CD spectrum. The SAXRD pattern illustrates that the gelator maintains a layered structure with an interlayer distance of 4.96 nm. Therefore, we propose that a 1D helical column with a clockwise direction is the basic structural building block of the organogel fibers. On the other hand, the fibrous structure of the organogel is successfully transcribed into silica fibers with unique 15 nm inner diameters by the sol−gel polycondensation of tetraethoxysilane in the gel phase. It is first found that the aggregation of the gelator can rearrange into a stable hexagonal structure to lead to the hollow silica fibers with 15 nm inner diameters due to the adsorption of the oligomeric silica species onto the incipient cationic organogel fibers during the sol−gel transcription.

Introduction

Recently, the construction of inorganic materials with order nanostructure is the subject of much attention because of their potential wide-ranging applications in catalysis, absorption, nanotechnology, etc. It is the perfect example that many molecules, such as synthetic polymers,[1] amphiphiles,[2] peptides[3] and DNA,[4] have been designed to self-assemble into ordered structures with novel useful properties, which may lead to diverse organic−inorganic composites or novel structural inorganic materials. Particularly, low-molecular-weight gelators have stimulated considerable interest[5] since most organogelators can assemble into nanoscale superstructures, such as fibers, rods, and ribbons, through weak noncovalent interactions (hydrogen bonding, $\pi-\pi$ interaction, van der Waals interaction, coordination, and charge-transfer interaction) to create three-dimensional networks which result in the gelation of organic solvent. Furthermore, organogels have been applied as templates to fabricate various nanostructures of SiO_2,[6] TiO_2,[7] Al_2O_3,[8] and CdS[9] with tubules, lamellar, helical fiber, and spherical morphologies. It is well-known that the organogelator with cationic charge is beneficial to the transcription of the organogel structure into the silica material in the sol−gel polycondensation of tetraethoxysilane (TEOS)[10] since the anionic oligomeric silica species can adsorb on the cationic gelator fibers

* To whom correspondence should be addressed. Fax: +86-431-8949334. E-mail: luran@mail.jlu.edu.cn.

† State Key Laboratory of Superhard Materials.

‡ College of Life Sciences.

(1) (a) Caruso, F. *Adv. Mater.* **2001**, *13*, 11−22. (b) Caruso, F. *Chem.−Eur. J.* **2000**, *6*, 413−419. (c) Reuter, T.; Vidoni, O.; Torma, V.; Schmid, G.; Nan, L.; Gleiche, M.; Chi, L.; Fuchs, H. *Nano Lett.* **2002**, *2*, 709−711.

(2) (a) Walsh, D.; Mann, S. *Nature* **1995**, *337*, 320−323. (b) Yada, M.; Kitamura, H.; Ichinose, A.; Machida, M.; Kijima, T. *Angew. Chem., Int. Ed.* **1999**, *38*, 3506−3510. (c) Yaha, M.; Mihare, M.; Mouri, S.; Kuroki, M.; Kijima, T. *Adv. Mater.* **2002**, *14*, 309−313. (d) Hartgerink, J. D.; Beniash, E.; Stupp, S. I. *Science* **2001**, *294*, 1684−1688.

(3) (a) Reches, M.; Gazit, E. *Science* **2003**, *300*, 625−627. (b) Fu, X.; Wang, Y.; Huang, L.; Sha, Y.; Gui, L.; Lai, L.; Tang, Y. *Adv. Mater.* **2003**, *15*, 902−906. (c) Azriel, R.; Gazit, E. *J. Biol. Chem.* **2001**, *176*, 34156−34161.

(4) (a) Richter, J.; Seidel, R.; Kirsch, R.; Mertig, M.; Pompe, W.; Plaschke, J.; Schackert, H. K. *Adv. Mater.* **2000**, *12*, 507−510. (b) Mertig, M.; Ciacchi, L. C.; Seidel, R.; Pompe, W. *Nano Lett.* **2002**, *2*, 841−844.

(5) (a) Terech, P.; Weiss, R. G. *Chem. Rev.* **1997**, *97*, 3133−3159. (b) Fuhrhop, J.-H.; Helfrich, W. *Chem. Rev.* **1993**, *93*, 1565−1582. (c) Bhattacharya, S.; Achrya, S. N. G. *Chem. Mater.* **1999**, *11*, 3121−3132. (d) Rowan, A. E.; Nolte, R. J. M. *Angew. Chem., Int. Ed.* **1998**, *37*, 63−68. (e) George, M.; Weiss, R. G. *Chem. Mater.* **2002**, *14*, 1445−1447. (f) Haines, S. R.; Harrison, R. G. *Chem. Commun.* **2002**, 2846−2847. (g) George, M.; Weiss, R. G. *Langmuir* **2003**, *19*, 1017−1025. (h) Estroff, L. A.; Hamilton, A. D. *Angew. Chem., Int. Ed.* **2000**, *39*, 3447−3450. (i) Placin, F.; Desvergne, J. P.; Lassegues, J. C. *Chem. Mater.* **2001**, *13*, 117−121. (j) Suzuki, M.; Yumoto, M.; Kimura, M.; Shirai, H.; Hanabusa, K. *Chem.−Eur. J.* **2003**, *9*, 348−354.

(6) (a) Jung, J. H.; Shinkai, S.; Shimizu, T. *Chem. Mater.* **2003**, *15*, 2141−2145. (b) Jung, J. H.; Ono, Y.; Sakurai, K.; Sano, M.; Shinkai, S. *J. Am. Chem. Soc.* **2000**, *122*, 8648−8656. (c) Jung, J. H.; Kobayashi, H.; Masuda, M.; Shimizu, T.; Shinkai, S. *J. Am. Chem. Soc.* **2001**, *123*, 8785−8789. (d) Sugiyasu, K.; Tamaru, S.; Takeuchi, M.; Berthier, D.; Huc, I.; Oda, R.; Shinkai, S. *Chem. Commun.* **2002**, 1212−1213. (e) Kobayashi, S.; Hamasaki, N.; Suzuki, M.; Kimura, M.; Shirai, H.; Hanabusa, K. *J. Am. Chem. Soc.* **2002**, *124*, 6550−6551. (f) Jung, J. H.; Ono, Y.; Hanabusa, K.; Shinkai, S. *J. Am. Chem. Soc.* **2000**, *122*, 5008−5009. (g) Jung, J. H.; Yoshida, K.; Shimizu, T. *Langmuir* **2002**, *18*, 8724−8727. (h) Becerril, J.; Burguete, M. I.; Escuder, B.; Luis, S. V.; Miravet, J. F.; Querol, M. *Chem. Commun.* **2002**, 738−739.

(7) Jung, J. H.; Kobayashi, H.; van Bommel, K. J. C.; Shinkai, S.; Shimizu, T. *Chem. Mater.* **2002**, *14*, 1445−1447.

(8) Llusar, M.; Pidol, L.; Roux, C.; Pozzo, J. L.; Sanchez, C. *Chem. Mater.* **2002**, *14*, 5124−5133.

(9) Sone, E. D.; Zubarev, E. R.; Stupp, S. I. *Angew. Chem., Int. Ed.* **2002**, *41*, 1705−1709.

10.1021/cm034863d CCC: $27.50
Published on Web 08/26/2004

Table 1. Gelation Properties of 1 in Organic Solvents[a]

entry	solvent	gelation	entry	solvent	gelation
1	alcohol	P	6	benzene	I
2	1-butanol	G(S)	7	cyclohexane	I
3	1-octanol	I	8	acetic acid	P
4	DMF	P	9	*n*-butyl acetate	P
5	DMSO	P			

[a] Gelation of **1**: G(S), supergel formed at a gelator concentration below 1.0 wt/vol %; P, precipitate, I, insoluble.

because of the electrostatic interaction and further polymerization may proceed according to the morphologies of the template. However, to date, the silica superstructures obtained by the template transcription of organogel assemblies have been characterized by the broad distribution, and the rearrangement of the aggregation of the organogelator during the transcription was not studied. To construct monodispersed silica fibers, we designed a new dimeric cholesterol-based cationic gelator (**1**) as the template. It was found that the gelator **1** could self-assemble into a fibrous aggregation in 1-butanol in which unimolecular stacking fibers with ca. 5 nm diameters twisted into thin fibers with 10 nm diameters in a clockwise direction. Meanwhile, the organogel fibers could be well transcribed into hollow fibrous silica with a monodispersed diameter of 15 nm, and the rearrangement of the aggregation of the gelator into a stable hexagonal structure during the sol−gel polycondensation of TEOS was first observed. We also found that the rate of sol−gel polycondensation of TEOS played a key role in the rearrangement of the aggregation of the gelator, so the silica or other fibers with different inner diameters could be generated controllably by simply adjusting the rate of sol−gel condensation.

Result and Discussion

Gelation Test. The gelation ability of **1** was estimated for different organic solvents including alcohol, aromatic solvents, DMF, DMSO, etc. As summarized in Table 1, it was found that **1** could form a stable gel only in 1-butanol among these solvents at a gelation concentration below 1.0 wt/vol %, called a supergel. The solubility of **1** was very poor; it could only be solubilized in some hot polar solvents, such as DMSO, ethanol, etc. Left-handed twist crystals with approximate 100 nm diameters could be formed after the ethanol solution was cooled (Figure 1). This indicated that **1** preferred to form a one-dimensional chiral fibrous structure in the crystal state, which may provide information on the gel structure, since they consisted of the same structural units as proved in the following sections.

Circular Dichroism (CD) Spectroscopy. CD spectroscopy can evaluate the aggregation of chiral molecules when chromophoric moieties are organized into a specific chiral orientation in the liquid or solid phase. Recently, CD spectroscopy has been used to characterize the aggregation mode in the organogel phase.[5a−c] Figure 2b shows the CD spectrum of organogel **1** in 1-butanol,

Figure 1. 1. Optical micrographs of the precipitate of **1** formed from ethanol.

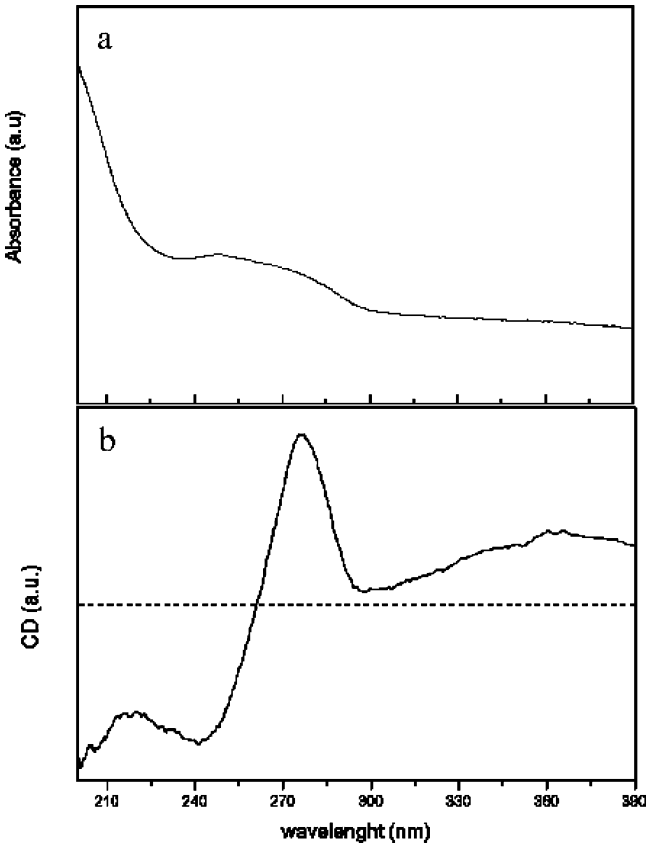

Figure 2. 2. Absorption (a) and CD (b) spectra for gel **1** in 1-butanol.

and we find that the $\lambda_{\theta=0}$ value appeared at 259 nm, which was consistent with the absorption maximum of **1** as shown in Figure 2a. The order of the bands, namely, positive at long wavelength and negative at short wavelength, was indicative of positive exciton-coupling bands for the Cotton effect, indicating that the dipole moments of **1** were orientated in a clockwise direction in the aggregation of the gelator.[5c,11]

Morphology of Xerogels As Examined by Polarized Light Microscopy and Transmission Electron Microscopy (TEM). From polarized light microscopy

(10) (a) van Bommel, K. J. C.; Shinkai, S. *Langmuir* **2002**, *18*, 4544−4548. (b) Ono, Y.; Nakashima, K.; Sano, M.; Hojo, J.; Shinkai, S. *J. Mater. Chem.* **2001**, *11*, 2412−2419. (c) Ono, Y.; Nakashima, K.; Sano, M.; Kanekiyo, Y.; Inoue, K.; Hojo, J.; Shinkai, S. *Chem. Commun.* **1998**, 1477−1478. (d) Jung, J. H.; Ono, Y.; Shinkai, S. *Chem.−Eur. J.* **2000**, *6*, 4552−4557.

(11) Wang, M.; Silva, G. L.; Armitage, B. A. *J. Am. Chem. Soc.* **2000**, *122*, 9977−9986.

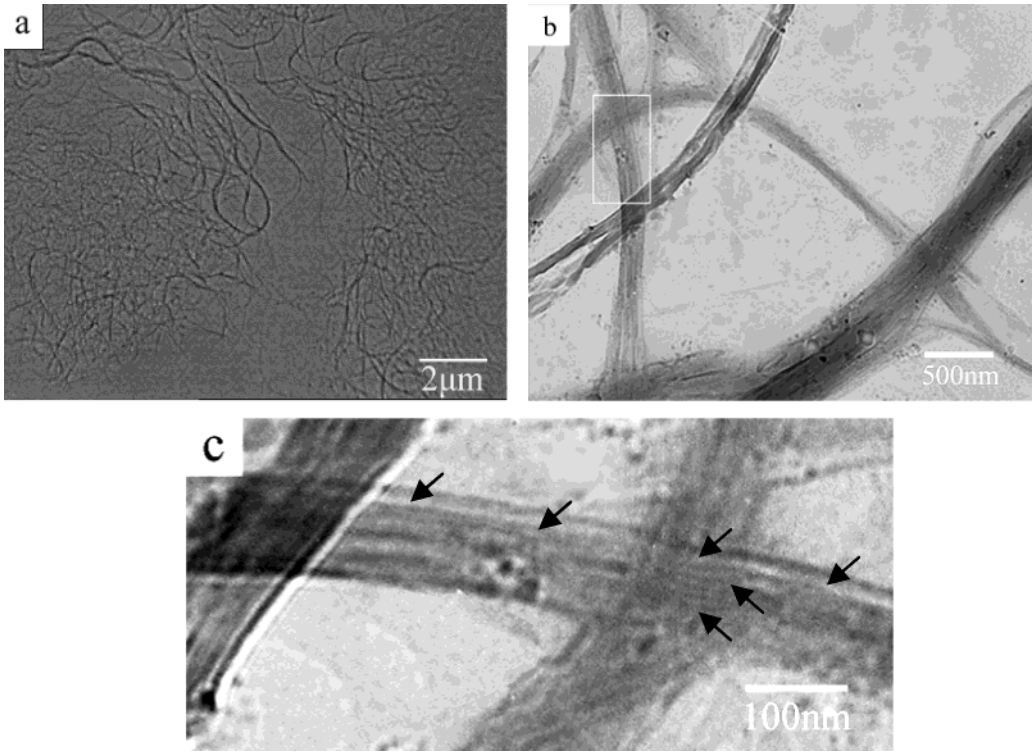

Figure 3. 3. (a) Optical micrographs of long and thick fibers of **1** in 1-butanol. (b) TEM image of gel **1**. The thick fibers consisted of long and thin fibers with 10 nm diameters, which are composed of two twisted fibers with 5 nm diameters. (c) High-magnification TEM image of the boxed region in (b).

and TEM pictures of xerogel **1**, we can observe the morphology of the xerogel. Figure 3a gives a polarized light microscopy picture of the xerogel **1** obtained from 1-butanol. It shows many long and thick fibers with lengths tens of micrometers and 100−500 nm diameters, and thick fibers composed of many thin fibers. To further canvas the microstructures of the fibers, TEM pictures of the xerogel **1** are shown in Figure 3b,c, which reveal that the thick fiber indeed consists of many thin fibers with unique diameters of 10 nm which were formed from two close fibers with ca. 5 nm diameters twisted together.

X-ray Diffraction. To reveal the molecular packing of gelators in the gel phase and the gelation mechanism,[12] X-ray diffraction patterns of the xerogel of **1** from a casting film of a wet gel are given in Figure 4a,b. Meanwhile, we obtained X-ray diffraction patterns of the neat crystal from ethanol, surprisingly, which were similar to those of the gel (Figure 4a,b). The slight difference was that the diffraction intensity of the crystal was stronger than that of the gel. This suggested that the molecular-packing mode in the organogel phase was the same as that in the crystal. The good diffraction pattern was characterized by four sharp reflection peaks of 4.96, 2.46, 1.64, and 1.21 nm (Figure 4a) in the low-angle region, the relative intensity of which was exactly in the ratio of 1:1/2:1/3:1/4. It illustrated that a perfect lamellar organization within the aggregates of gel **1** was formed and the interlayer distance of 4.96 nm corresponded to the diameter of the fibers (ca. 5 nm) observed in TEM. Furthermore, the appearance of several strong sharp peaks in the high-angle region could also indicate the highly ordered structure in the gel state.

Molecular Packing. The X-ray diffraction of gel **1** in the low-angle region suggested that the gel fibers consisted of multiple monolayers with a period of 4.96 nm. From the CPK molecular modeling, the fully extended molecular length of **1** was estimated to be 5.76 nm. The *d* value was shorter than the calculated length of the LMOGs in their extended linear conformation, and the helical fibers with ca. 5 nm diameters could be found in the TEM image, so we can see that the fibrous gel was constructed from a lamellar organization in which the molecules are arranged with tilting to the normal of the layer plane (Figure 5a). In view of the result of CD spectroscopy, which indicated that the dipole moments were orientated in a clockwise direction in the aggregation of the gelator, and the fact that the strong electrostatic interaction between viologen moieties made it impossible that **1** in the organogel adopted a folded conformation to enjoy efficient intramolecular and intermolecular cholesterol−cholesterol interaction,[5a,c,13] a one-dimensional helical column with a clockwise direction could be generated via the self-assembly of compound **1** in the gel state, in which viologen moieties formed a one-dimensional central column because of strong electrostatic interaction (Fig-

(12) (a) Shimizu, T.; Masuda, M. *J. Am. Chem. Soc.* **1997**, *119*, 2812−2818. (b) Imae, T.; Hayashi, N.; Matsumoto, T.; Tada, T.; Furusaka, M. *J. Colloid Interface Sci.* **2000**, *225*, 285−290. (d) Luo, X. Z.; Li, C.; Liang, Y. Q. *Chem. Commun.* **2000**, 2091−2092. (e) Masuda, M.; Hanada, T.; Okada, Y.; Yase, K.; Shimizu, T. *Macromolecules* **2000**, *33*, 9233−9238. (f) Jung, J. H.; John, G.; Masuda, M.; Yoshida, K.; Shinkai, S.; Shimizu, T. *Langmuir* **2002**, *17*, 7229−7232. (g) Jung, J. H.; Shinkai, S.; Shimizu, T. *Chem.—Eur. J.* **2002**, *8*, 2684−2690. (h) Zubarev, E. R.; Pralle, M. U.; Sone, E. D.; Stupp, S. I. *Adv. Mater.* **2002**, *14*, 198−203.

(13) Murata, K.; Aoki, M.; Suzuk, T.; Harada, T.; Kawabata, H.; Komori, T.; Ohseto, F.; Ueda, K.; Shinkai, S. *J. Am. Chem. Soc.* **1994**, *116*, 6664−6676.

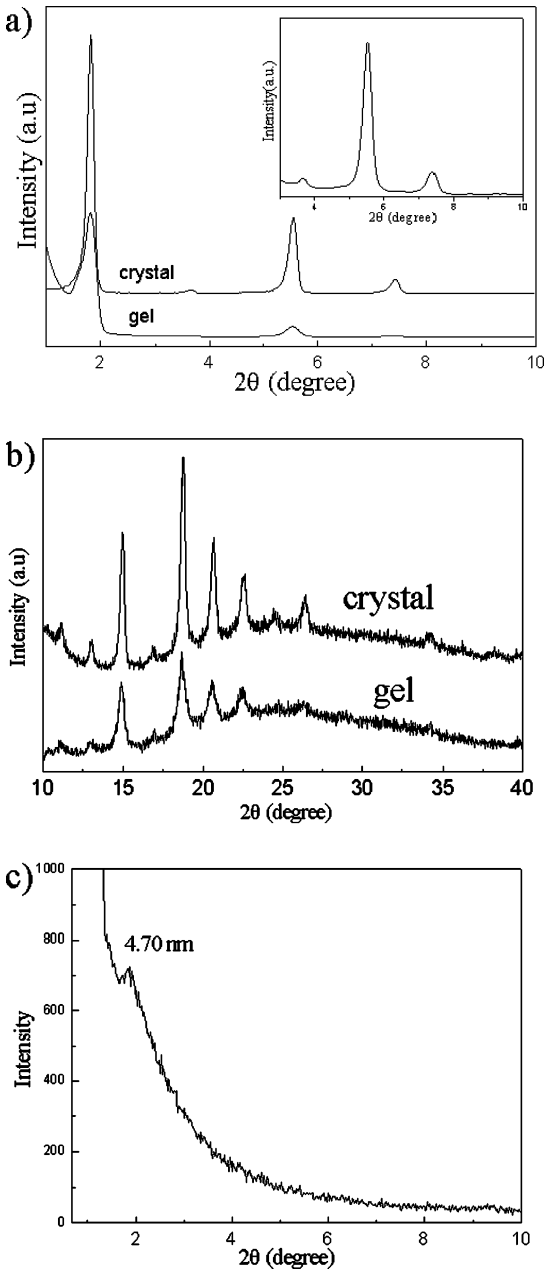

Figure 4. 4. X-ray diffraction patterns (room temperature) for (a) a gel and a crystal of **1** in the low-angle region (the inset shows the magnification pattern of the gel from 3° to 10°), (b) a gel and a crystal of **1** in the high-angle region, and (c) silica fibers without calcination obtained from method A in the low-angle region.

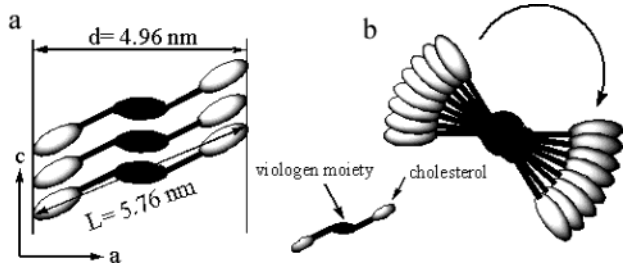

Figure 5. 5. Possible molecular packing for (a) a front view showing arrangement with tilting to the normal to the layer plane and (b) a one-dimensional aggregate model of **1**.

ure 5b). It was also deemed that the formation of the twist crystals from ethanol would be reasonable if the molecules stacked in the same mode as in the gel state, which was proved by X-ray diffraction (XRD). Therefore, the mode of molecular packing in the gel state was logical.

Sol−Gel Polycondensation of TEOS for Transcription. To transcribe the fibers formed in the organogel into the silica nanostructure, we carried out sol−gel polycondensation of TEOS using 1-butanol gel **1** as template according to the method described in the Experimental Section. The typical mixture consisted of 1-butanol, TEOS, water, and benzylamine as catalyst (method A). It was clearly seen from the TEM image (Figure 6a) that the silica without calcination showed a fibrous structure with an approximate 20−30 nm outer diameter and a unique hollow 15 nm inner diameter. Therefore, we can conclude that the organogel fibers act as an efficient template to transcribe the organic aggregate superstructure into the inorganic silica material. It is well-known that the silica propagation species were considered to be anionic when the sol−gel polycondensation was catalyzed with amine.[5a,10b] Hence, the oligomeric silica species could be adsorbed onto the cationic gelator fibers owing to the electrostatic interaction, and further polycondensation would proceed along these fibrils. This propagation mode provided a sort of organogel−silica gel composite fiber, which eventually generated a tubular structure.

To identify the effect of the electrostatic interaction between the cationic organogel fibers and the oligomeric silica species on the growth of fibrous silica, sol−gel polycondensation was carried out under various pH systems. It was found that the silica always showed the conventional sphere morphology in the organogel system using aqueous HCl or acetic acid as catalyst, which implied that TEOS polycondensation proceeded randomly and had no relationship to the presence of gelator fibers, since in the acid matrix the silica particles were no longer anionic,[10b] and unable to adsorb onto the cationic gelator fibers. The result obtained herein confirms that the electrostatic interaction played an indispensable role in the construction of the novel fibrous silica structure templated by organogel **1**.

Why is the inner diameter of the silica fiber generated by method A 15 nm and not 10 nm, which is comparable with that of the organogel fibers? This can be explained that during the adsorption of the oligomeric silica species onto the gelator fibers the rearrangement of the aggregation of organogel fibers occurs. In an attempt to provide further confirmation of this hypothesis, we investigated the effect of the rate of polycondensation of TEOS on the growth of silica fibers through controlling the heating time after injection of catalyst. This could regulate the quantum of anionic oligomeric silica before the formation of the gel fibers during the cooling.[14] Therefore, in method B, the solution was cooled fast by a cool water stream after the catalyst (benzylamine) was injected into the hot solution. The TEM image (Figure 6b) showed that the organogel of **1** could also result in fibrous silica with inner diameters of 15 nm; in addition, fibers with diameters of 10 and 5 nm appeared. One can estimate that the fibers with 15 nm diameters were the same as those obtained from method A; however, the silica tubules with inner diameters of

(14) Tamaru, S. I.; Takeuchi, M.; Sano, M.; Shinkai, S. *Angew. Chem., Int. Ed.* **2002**, *41*, 853−856.

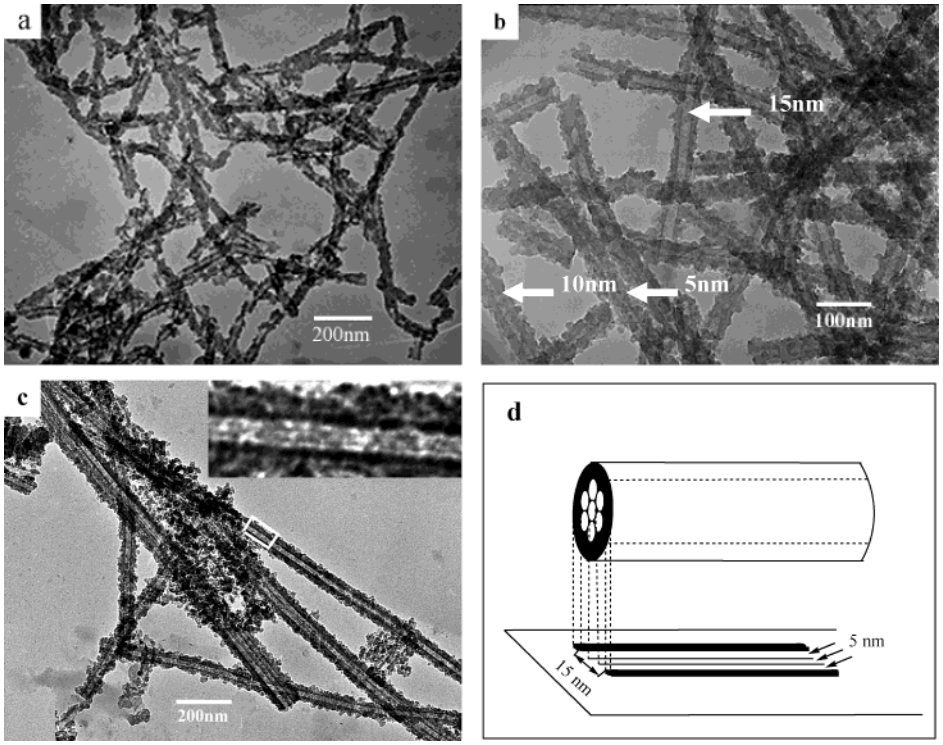

Figure 6. 6. TEM images of the silica obtained from (a) method A, (b) method B, and (c) method C. (d) Schematic representation of the fabrication of the fibrous silica with two stripes in the inner tube because of the hexagonal arrangement of the unimolecular stacking fibers of **1**.

10 and 5 nm were consistent with the diameter of the neat organogel fibers of **1** in 1-butanol as shown in Figure 3. We propose that the silica fibers with 10 and 5 nm inner diameters resulted from direct transcription of the organogel fibers with 10 and 5 nm diameters, respectively, without further rearrangement because the relatively lower rate of polycondensation of TEOS caused not enough anionic oligomeric silica species to adsorb onto the cationic fibers. The above results prove that the adsorptions of oligomeric silica species onto organogel fibers had an effect on the rearrangement of the fibers.

Whereafter, to demonstrate the rearrangement mode of the organogel fibers during the formation of the gel fibers, we prolong the heating time after injection of catalyst. For example, in method C, the solution was kept at 80 °C for 20 s after catalyst was injected into the hot solution, which could accelerate the sol−gel polycondensation of TEOS and increase the amount of oligomeric silica species and the degree of sol−gel polycondensation of TEOS. From the TEM image of Figure 6c silica fibers with 15−45 nm inner diameters and 40−100 nm outer diameters were obtained. Furthermore, the silica fibers were composed of microtubules with 5−17 nm diameters. With careful examination, we find that the silica fibers with 15 nm inner diameters bore two stripes which comparted the silica inner tubule into three portions with about 5 nm diameters, as shown in the inset of Figure 6c. And the silica fibers with a larger inner diameter were composed of two or three tubules with 15 nm inner diameters bearing stripes or a bundle of individual channels with 5 nm diameters. These results consistently support the point that the incipient organogel fibers with 5 nm diameters were encapsulated by small oligomeric silica species because of the higher rate of sol−gel polycondensation of TEOS. The reason the inner diameter of the silica tubules is not 10 nm, but 15 nm as obtained in method A, was that the rearrangement of the aggregation of **1** occurred during the adsorption of the oligomeric silica species onto the gelator fibers. It was deduced that six fibers with 5 nm inner diameters tended to rearrange into a stable hexagonal packing mode when the hot solution was cooled (Figure 6d) and the self-assembled stable organogel could be transcribed into the stable unique hollow silica fibers with 15 nm inner diameters observed in the TEM pictures. The X-ray diffraction pattern of the silica without calcination from method A showed one clear reflection at 4.70 nm in the low-angle region (Figure 4c). If the hypothesis of the rearrangement into a stable hexagonal packing mode were credible, the diameter of a column of the columnar phase would be confirmed as $4.70/\cos 30° = 5.43$ nm, which is in reasonable agreement with the diameter (ca. 5 nm) of the gel fibers. The slightly larger diameter (5.43 nm) of the column was due to the absorption of the oligomeric silica species onto the gelator fibers. This result also supports the hypothesis of the rearrangement mechanism.

Conclusion

In conclusion, dimeric cholesterol-based viologen derivative **1** could self-assemble into a fibrous supergel in 1-butanol, and such organogel fibers can be used as a good template for construction of monodispersed hollow fibrous silica. It was found that the inner diameter of the obtained silica fibers was 15 nm, which is not consistent with that of the organogel fiber. This phenomenon can be explained by the fact that the aggregation of the gelator could rearrange into a stable hexagonal structure during the formation of the gel fibers due to the adsorption of anionic oligomeric silica species

Scheme 1

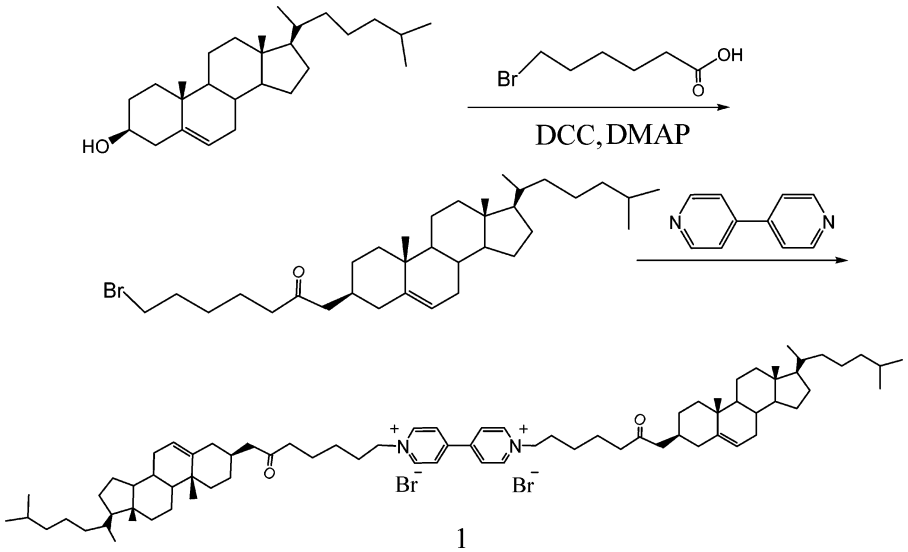

1

onto cationic gel fibers. Therefore, one could fabricate silica fibers with different inner diameters via simply adjusting the rate of sol−gel polycondensation.

Experimental Section

Instruments. Infrared spectra were measured using a Nicolet-360 FT-IR spectrometer by incorporating samples in KBr disks. ^{1}H nuclear magnetic resonance (^{1}H NMR) spectra were measured on a Varian 300 MHz FT-NMR spectrometer. The UV−vis absorption spectra were determined on a Shimadzu-1601 spectrophotometer. C, H, and N elemental analyses were performed on a Perkin-Elmer 240C elemental analyzer.

CD Spectroscopy. The CD spectrum of organogel **1** in 1-butanol was recorded on a JASCO J-715 spectropolarimeter. The spectrum was measured with a thin membrane prepared by sandwiching the sample gel between two quartz slides, and the contribution of LD (linear dichroism) was confirmed to be negligible.

TEM Measurement. A piece of the neat gel of **1** in 1-butanol was placed on a carbon-coated copper grid (400 mesh) followed by natural evaporation of the solvent. Then the sample was dried completely for **1** h at low pressure. The specimens were examined with a Hitachi mode H600A-2 apparatus with an accelerating voltage of 100 kV.

Gelation Test of Organic Fluids. The solution mixture of the weighed gelator in organic solvent was heated in a sealed test tube in an oil bath until the solid was dissolved. After the solution was allowed to stand at room temperature for 6 h, the state of the solution was evaluated by the "stable to inversion of a test tube" method.

XRD. Diffraction patterns were carried out on a Rigaku D/max-rA X-ray diffractometer with graphite-monochromatized Cu Kα radiation ($\lambda = 1.5418$ Å). The accelerating voltage was set at 50 KV, with 100 mA flux at a scanning rate of 0.05 deg/s in the 2θ range of 10−40° for high-angle diffraction patterns and 0.02 deg/s in the 2θ range of 0.7−10°. The samples were prepared by packing about 5 mg of solid in a standard cavity mount, and a piece of the neat gel of **1** in 1-butanol was placed on a silicon flake.

Sol−Gel Polycondensation. *Method A*. Gelator **1** (2.0−3.0 mg) was added to the mixed solution of BnOH (800 μL), DMF (200 μL), water (6 μL), and TEOS (20 μL), and the mixture was heated until the precipitate was dissolved completely. $BzlNH_2$ (5 μL) as catalyst was added immediately, and then the solution was cooled unaffectedly to room temperature. This reaction mixture was placed in the dark for 7 days. The product was washed with ethanol and dried in vacuo to give an organic−inorganic composite.

Method B. The preparation process of the reaction mixture was the same as that in method A, but the mixture was cooled immediately by a cool water stream after $BzlNH_2$ (5μL) was added.

Method C. The preparation process of the reaction mixture was also the same as that in method A. After $BzlNH_2$ (5 μL) was added, the mixture was heated at 80 °C for an additional 20 s.

Preparation of the Cholesterol-Based Organogelator. The organogelator 1 was synthesized as shown in Scheme 1, and the detailed methods are described below.

Cholesteryl 6-Bromocaproate. 6-Bromohexanoic acid (2.1 g, 10.25 mmol) and cholesterol (3.87 g, 10 mmol) were dissolved in 40 mL of dry dichloromethane under a nitrogen atmosphere. The solution was maintained at 0 °C by an ice bath, and then dicyclohexylcarbodiimide (DCC; 2.06 g, 10 mmol) and (dimethylamino)pyridine (DMAP; 0.21 g, 1 mmol) were added. The reaction mixture then was stirred for 4 h at 0 °C and 12 h at room temperature. The precipitate was filtered and removed, and the filtrate was washed with 10% hydrochloric acid and 5% sodium bicarbonate aqueous solution. The organic layer then was dried by sodium sulfate and evaporated to dryness. The residue was purified by a silica gel column eluting with ethyl acetate/cyclohexane (1:6, v/v) to obtain the product at 34% yield as a colorless solid: mp 116−118 °C; ^{1}H NMR (300 MHz, $CDCl_3$, TMS) $\delta = 5.37$ (1H, d, $J = 4.8$), 4.65−4.56 (1H, m), 3.41 (2H, t, $J = 6.9$), 2.30 (4H, t, $J = 7.5$), 2.1−0.6 (47H, m); IR (KBr) $\tilde{\nu} = 2934-2867$, 1733, 1465 cm^{-1}. Anal. Calcd for $C_{33}H_{55}BrO_2$ (563.69): C, 70.31; H, 9.83. Found: C, 70.19; H, 10.01.

4,4′-(Bis(6-cholesteryloxy)carbonylpentyl)bipyridinium Bromide. A mixture of cholesteryl 6-bromocaproate (1.127 g, 2.0 mmol) and 4,4′-bipydidine (0.192 g, 1.0 mmol) was refluxed in dry acetonitrile (100 mL) for 48 h. After cooling to room temperature, the yellow insoluble compound was filtered. The product was obtained by two recrystallizations from ethanol: yield 37%; mp > 300 °C; ^{1}H NMR (300 MHz, [D_6]DMSO, TMS) $\delta = 9.40$ (4H, d, $J = 6.9$), 8.80 (4H, d, $J = 6.6$), 5.31 (2H, d, $J = 3.2$), 4.68 (4H, t, $J = 6.9$), 4.51−4.42 (2H, m), 2.4−0.5 (94H, m); IR (KBr): $\tilde{\nu} = 3046$, 2934, 2866, 2845, 1728, 1639, 1465, 1447 cm^{-1}. Anal. Calcd for $C_{76}H_{118}Br_2N_2O_4$ (1283.57): C, 71.12; H, 9.27; N, 2.18. Found: C, 70.83; H, 9.24; N, 2.23.

Acknowledgment. We acknowledge the National Nature Science Foundation of China (NNSFC) for financial support of this work.

CM034863D